J. Environ. Nanotechnol.
Volume 2, No.4 pp.51-56
ISSN (Print) : 2279-0748
ISSN (Online) : 2319-5541
doi : 10.13074/jent.2013.12.132051

Fabrication of Hyddrophobic ZnO Surfaces on SS304 Substrates

R. Amiruddin[1], Akshay Srinivas[2], C. S. Sujith Kumar[3], M. C. Santhosh Kumar[4]*

[1,2,4*]*Department of Physics, National Institute of Technology, Tiruchirappalli, TN, India.*
[3]*Department of Mechanical Engineering, National Institute of Technology, Tiruchirappalli, TN, India.*

Received: 20.07.2013 Accepted: 24.12.2013

Abstract

We have deposited undoped ZnO and 3% Al doped ZnO layers upon stainless steel (SS 304) substrates to study the hydrophobic nature of the surface. The ZnO layers were deposited at 673K by spray pyrolysis. Then the prepared films were annealed at various temperature like 723K, 773K, 873K and 973K. The structural and compositional analysis shows that the ZnO has a preferential growth along (002) planes. By contact angle measurement, it is revealed that annealed samples at 723K for both ZnO as well as 3% Al doped ZnO surfaces exhibits maximum contact angle of 120.59° and 125.97° respectively, which shows that the surfaces are hydrophobic. The photoluminescence spectra show that there are blue and green emission peaks in all samples. Thus, the hydrophobic ZnO thin films can be of great importance in commercial application as transparent self-cleaning surfaces.

Keywords: *Contact angle; Hydrophobicity; ZnO.*

1. INTRODUCTION

The superhydrophobic surfaces have received much attention due to their importance in fundamental research and promising applications such as lenses, transparent window glasses, textiles (Feng *et al.* 2006), self-cleaning materials, antifog, anti-snow, fluid microchips and microreactors(Richard *et al.*2002; Erbil *et al.* 2003). The concept of super hydrophobic surfaces is originally inspired from the lotus leaves. The "lotus effect" refers to the high water repellency and the self-cleaning property of lotus leave. This effect has been attributed to the combine effect of hydrophobicity induced in the epicuticular wax and surface resulted from hierarchical structure. On a chemically homogeneous and a physically flat surface the surface wettability depends on the chemical composition. The liquid contact angle depends on the interfacial free energies, i.e free energies at the solid-air (γSV), solid-liquid (γSL) and the liquid-air (γLV) interface by the Young's equation,

$$\cos\theta = \frac{\gamma SV - \gamma SL}{\gamma LV}$$

The solid surface is considered to be intrinsically hydrophobic if the contact angle is greater than 90º and the solid surface is considered intrinsically hydrophilic when θ is less than 90º. The reported lowest surface free energy of the solid air interface is possessed by the fluoromethyl group terminated surface. By manipulating the surface topography the hydrophobicity of the surface can be improved. Generally wetting regimes have been classified into three distinct states such as the cassie state, the weznel state and the intermediate state. The weznel state describes the situation where a liquid drop penetrates into the groves of the surface whereas the cassie state describes the situation where a drop rests on the surface without

***M. C. Santhosh Kumar**
E-mail: santhoshmc@nitt.edu

penetration (Bico *et al.* 2002 and Sik Park *et al.* 2008). The relationship between the apparent contact angle on a rough surface and the intrinsic contact angle has been described by the weznel equation

$$\cos \theta_w = \cos \theta_y$$

where 'r' is the roughness factor, θ_w is the Weznel angle and θ_y is the cassie angle. It is the ratio of the actual surface area to its horizontal projection.

2. EXPERIMENT

Two sets of hydrophobic layers were deposited and analyzed. The first one is ZnO layers and the other being the optimized Al 3 at % doped ZnO layers. Both these layers were deposited upon the stainless steel (SS 304) substrates. A solution of 0.1 M of zinc acetate (Sigma-Aldrich, 99.5%, Germany) was prepared by dissolving it in deionized water and 10ml ethanol (Merck, 99.9%, Germany). The solution was stirred for few minutes. Few drops of acetic acid are added to make the solution transparent and homogenous. The solution was then sprayed on to the SS 304 substrate which is placed on the base heated at 673K. Compressed air is used as the carrier gas.When the aerosol droplets come close to the substrates, a pyrolytic process occurs and highly adherent films were produced. The substrate temperature is maintained at 673K which is controlled by the temperature controller.

The distance between the spray nozzle and the substrates were maintained at 15 cm. Compressed air with an optimum pressure of 3 torr is used as an atomizer, which helps in spraying the solution uniformly in a smooth shower like manner over the preheated substrates. The deposition rate is 8 ml/min. The coating duration is 6 mins and four layers of coatings were carried out. The deposited samples were annealed at temperatures 723 K, 773 K, 873 K, 973 K. And for the preparation of Al 3 at % doped ZnO layers, aluminium Chloride hexahydrate (Sigma-Aldrich, 99.5%, Germany) is used as a precursor. The deposition conditions of Al 3% doped ZnO layers were same as for the deposition of undoped ZnO layers. The thickness of the deposited layers were measured by Stylus Profilometer and found to be 1.80 (microns).

3. RESULTS & DISCUSSION

3.1 Structural Analysis

Fig.1 shows the X-ray diffraction analysis of the undoped ZnO layers. The x-ray diffraction patterns were recorded for 2θ varying from 20º to 80º. It is observed that the film exhibits single phase wurtzite structure of ZnO and has a plane of reflections in the direction (002), (101), (100), (103), (112) and (102). The peaks observed are in good agreement with the standard values taken from JCPDS card number 75-0576. The preferential orientation of the formed films is along the (002) reflection plane. Thus all the films are highly oriented along the c-axis. The crystallite size of the films was calculated using the Scherrer's formula:

$$D = \frac{k\lambda}{\beta \cos\theta}$$

where λ is the wavelength of CuK_α radiation (1.5406 Å), k is shape factor (0.9), θ is the Bragg's diffraction angle and β is the broadening of the diffraction β line (FWHM). Fig.1 shows the XRD pattern of undoped ZnO layers for unannealed and also for different annealing temperature such as 723 K, 773 K, 873 K, 973 K. The SS 304 substrate XRD peaks are also shown in Fig.1. Initially, the steel has both ferrite and the austenite phase. Ferrite (α) corresponds to the BCC lattice and the austenite (γ) corresponds to FCC lattice. The austenite phase becomes more prominent when the sample annealing temperature is increased. This SS 304 substrates peak matches with JCPDS card numbers 34-0396 and 33-0397. Fig.2 shows the XRD pattern of optimized Al 3% doped ZnO layers for the same annealing parameters. The XRD peak intensity is maximum for unannealed samples and the intensity decreases when the annealing temperature is increased.

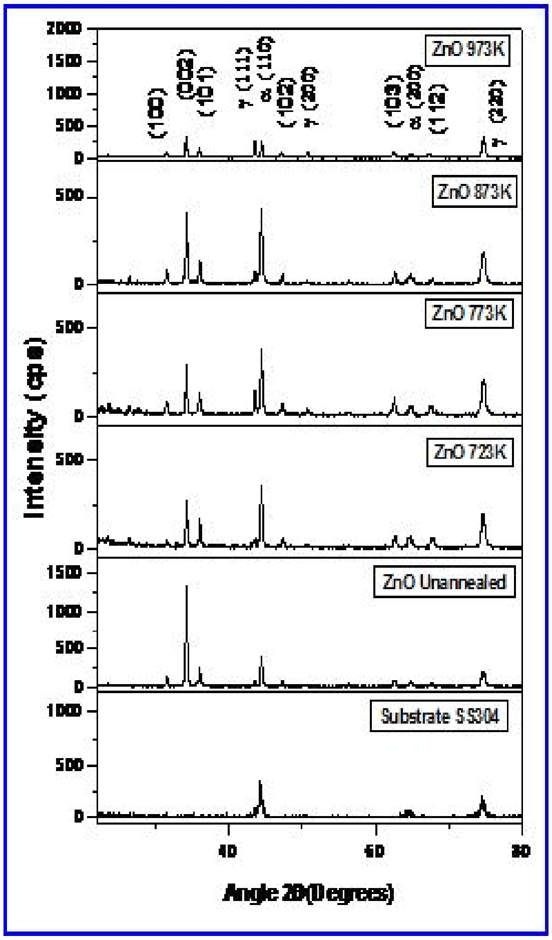

Fig. 1 : XRD pattern of undoped ZnO layers upon SS 304 substrates

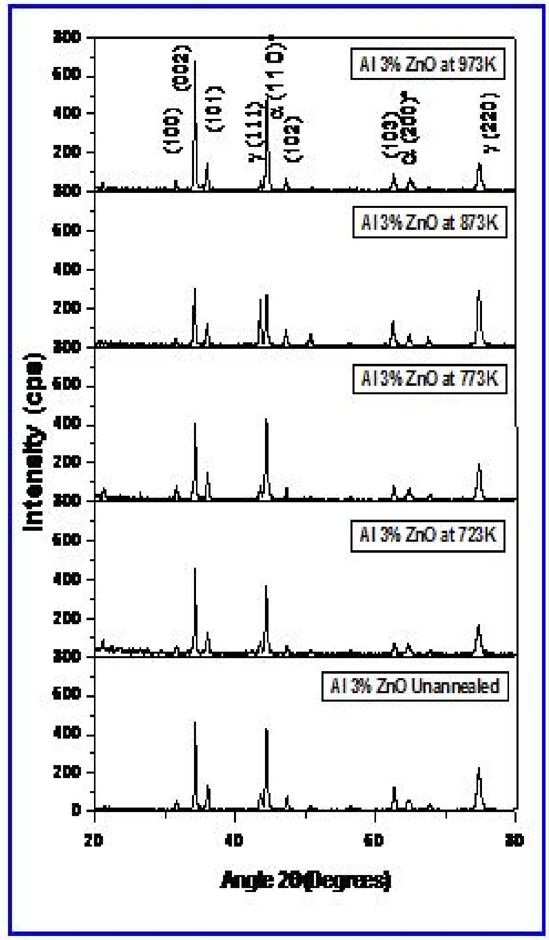

Fig. 2 : XRD pattern of Al 3% doped ZnO layers for different annealing temperature such as 723K, 773K, 873K and 973K. (where Ferrite ( ) and austenite ( ) phases corresponds to the SS 304 substrate peaks)

However the change in intensity for different annealing temperature is comparatively less.

3.2 Contact angle measurement

The contact angle (CA) measurement of water upon the coated surfaces was measured by contact angle meter (HOLMARC). Fig.3 and Fig.4 shows the water contact measurement for ZnO layers and Al doped ZnO layers upon the stainless steel substrate. It is revealed that the water contact angle (CA) for the surfaces which are annealed at 723 K exhibits the maximum contact angle for undoped ZnO and Al doped ZnO layers. The undoped ZnO surface which is annealed at 723 K shows contact angle (CA) of 120.59º whereas the Al 3 % doped ZnO surface annealed at 723 K shows 125.97º. These results shows that the fabricated ZnO and Al doped ZnO surfaces shows hydrophobic surface (CA > 90º).

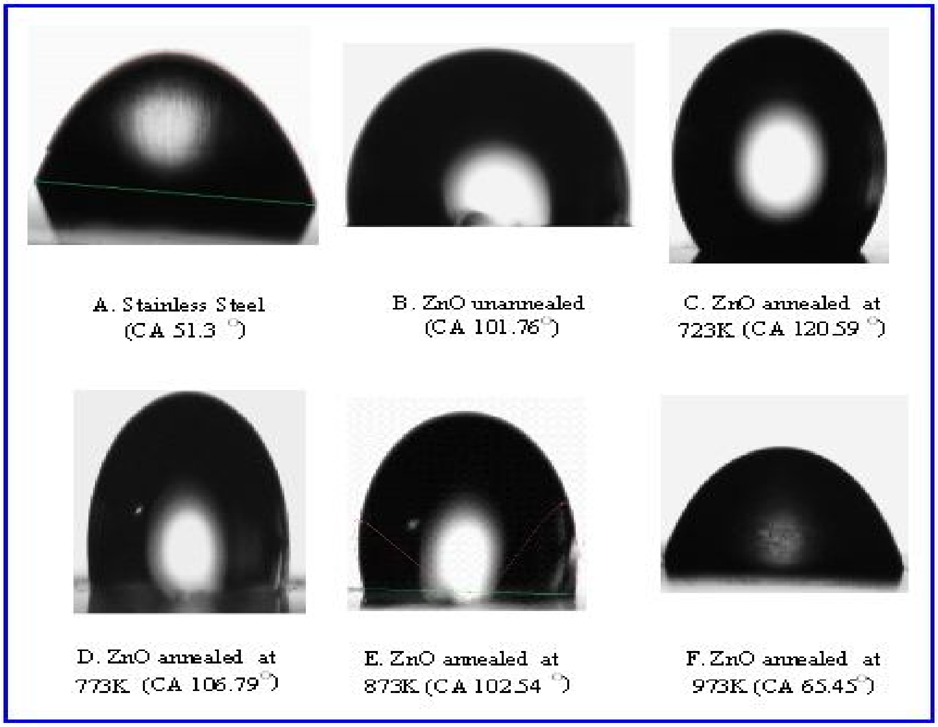

Fig. 3: Contact Angle(CA) of (A) Stainless Steel; (B) ZnO unannealed; (C) ZnO annealed at 723K; (D) ZnO annealed at 773K; (E) ZnO annealed at 873K; (F) ZnO annealed at 973K

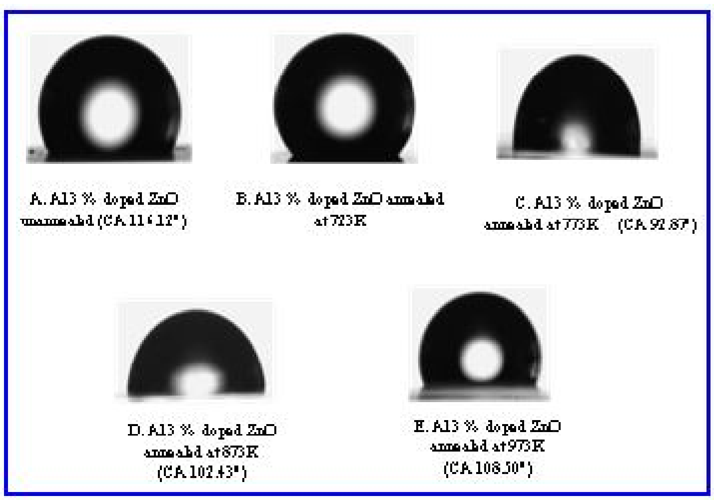

Fig. 4: Contact Angle(CA) of (A) Al 3% doped ZnO unannealed; (B) Al 3% doped ZnO annealed at 723K; (C) Al 3% doped ZnO annealed at 773K; (D) Al 3% doped ZnO annealed at 873K; (E) Al 3% doped ZnO annealed at 973K

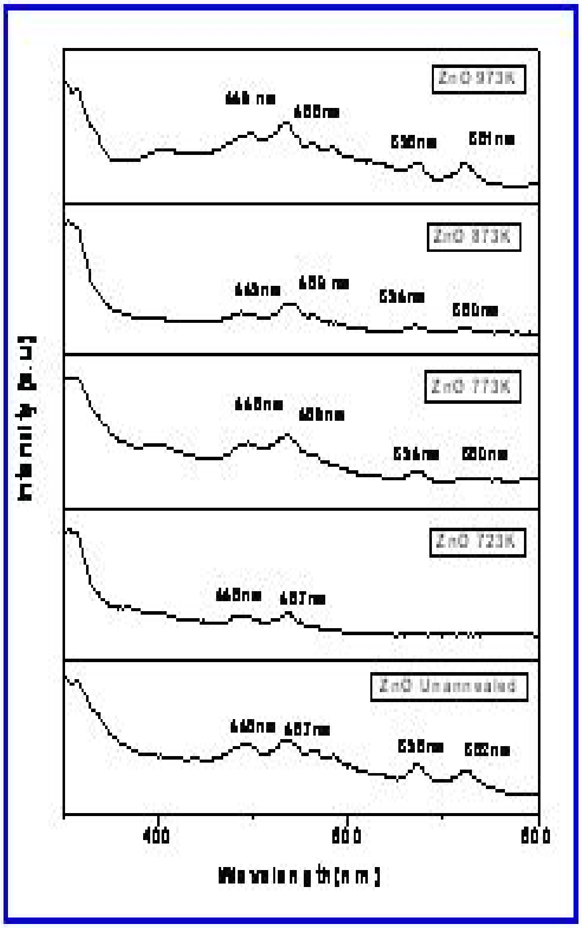

Fig. 5: Photoluminiscence analysis of undoped ZnO layers upon SS 304 substrates

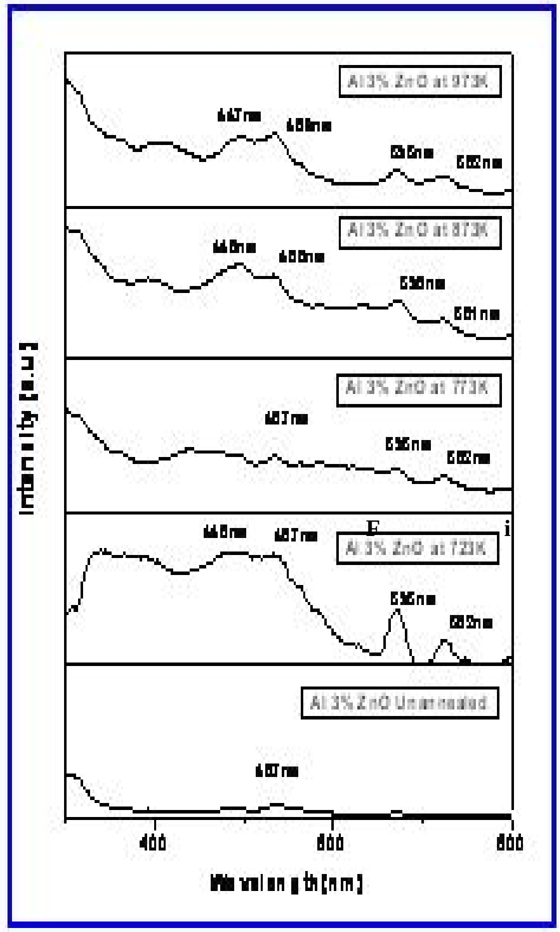

Fig. 6: Photoluminescence analysis of Al 3% doped ZnO layers for different annealing temperature such as 723K, 773K, 873K and 973K

3.3 Photoluminescence Studies

Photoluminescence spectra were recorded at room temperature with an excitation wavelength of 325 nm. Fig.5 and Fig.6 shows the photoluminescence studies of undoped ZnO layers and Al 3 at % doped ZnO layers upon the SS304 substrates. The UV region relates to free exciton recombination and the visible region reveals the deep level emission. This deep level emission is attributed to structural defects such as oxygen vacancies and interstitial zinc. Both the doped and the undoped annealed samples exhibit emission peaks in and around 445 nm, 469 nm, 534 nm, 560 nm. The peaks corresponding to 445 nm and 469 nm are blue emission peaks. The peaks at 534 nm are attributed to the presence of interstitial oxygen defects.

4. CONCLUSION

In summary, rough structures consisting of simple zinc ions surfaces, can enhance the wettability of the surface, and create both Cassie and Wenzel type

surfaces. By depositing ZnO layers and Al doped ZnO layers the water contact angle (CA) which is achieved are 120.570 and 125.970 respectively. These values show that the obtained surfaces exhibit hydrophobic surfaces. The hydrophobic ZnO thin films can be of great importance in commercial application as transparent self-cleaning surfaces. However, the superhydrophobic surface with contact angle (CA) exceeding 1500 can be possible to achieve when the initial molarity concentration of the ZnO is increased (Tarwal *et al*. 2010) and also when the deposited layers are modified further with some low surface energy materials like fluoroalkylsilane (FAS) (Li *et al*. 2005). The other possibility of developing superhydrophobic surfaces based on ZnO is to fabricate vertically aligned closely packed one dimensional nanostructures upon the substrates.

REFERENCES

Bico, J., Thiele, U. and Quere, D., Wetting of textured surfaces, Colloids and Surfaces A: Physicochem. *Engn, Aspects.*, 206,41-46(2002). http://dx.doi.org/10.1016/S0927-7757(02)00061-4.

Erbil, H. Y., Demire, A. L, Avci, Y., Mert, O. , Transformation of a Simple Plastic into a Superhydrophobic Surface, *Science.*, 299, *1377-1380(2003)*. *http://dx.doi.org/10.1126/science.1078365*.

Feng, X. J., Jiang, L., Design and Creation of Superwetting/Antiwetting Surfaces, *Adv. Mater.*, 18, 3063–3078(2006). http://dx.doi.org/10.1002/adma.200501961.

Li, Y., Cai, W., Duan, G., Cao, B., Sun, F., Lu, F., Superhydrophobicity of 2D ZnO ordered pore arrays formed by solution-dipping template method, *J. Colloid Interface Sci.*, 287, 634-639(2005). http://dx.doi.org/10.1016/j.jcis.2005.02.010.

Richard, D., Clanet, C., Quere, D., Brief Communications-Surface phenomena: Contact time of a bouncing drop, *Nature.*, 417, 811(2002). http://dx.doi.org/10.1038/417811a.

Sik Park, S., Lee, J. M., Kim. S. J. and Kim, S. W., *Journal of the Korean Physical Society.*, 53, 183(2008).

Tarwal, N. L. and Patil, P. S., Superhydrophobic and transparent ZnO thin films synthesized by spray pyrolysis technique, *Appl. Surf. Sci.*, 256, 7451(2010). http://dx.doi.org/10.1016/j.apsusc.2010.05.089.